Hindawi Publishing Corporation
Mobile Information Systems
Volume 2016, Article ID 9754162, 10 pages
http://dx.doi.org/10.1155/2016/9754162

Research Article

Feature-Based Digital Modulation Recognition Using Compressive Sampling

Zhuo Sun, Sese Wang, and Xuantong Chen

Beijing University of Posts and Telecommunications, Beijing 100876, China

Correspondence should be addressed to Zhuo Sun; zhuosun@bupt.edu.cn

Received 2 November 2015; Accepted 8 December 2015

Academic Editor: Qilian Liang

Compressive sensing theory can be applied to reconstruct the signal with far fewer measurements than what is usually considered necessary, while in many scenarios, such as spectrum detection and modulation recognition, we only expect to acquire useful characteristics rather than the original signals, where selecting the feature with sparsity becomes the main challenge. With the aim of digital modulation recognition, the paper mainly constructs two features which can be recovered directly from compressive samples. The two features are the spectrum of received data and its nonlinear transformation and the compositional feature of multiple high-order moments of the received data; both of them have desired sparsity required for reconstruction from subsamples. Recognition of multiple frequency shift keying, multiple phase shift keying, and multiple quadrature amplitude modulation are considered in our paper and implemented in a unified procedure. Simulation shows that the two identification features can work effectively in the digital modulation recognition, even at a relatively low signal-to-noise ratio.

1. Introduction

Constantly increasing volume of data transmitted through the mobile communication networks and the needs of users to increase the data rates lead to rapid development of mobile communication systems. The future fifth generation (5G) wireless communication tends to achieve a remarkable breakthrough both in data rate and spectral efficiency [1]. With demand for large data size and high data rate, vast spectrum resources are required urgently. However, most spectrum resources below 2G are fixedly occupied by other industries, although they have not been fully utilized. Considering this, the purpose of spectrum sensing in mobile communication networks is to share spectrum resources with other industries, without interfering with their normal operations. Moreover, spectrum sensing can be also applied to coordinate the public resources, which is a revolutionary change of the fixed spectrum allocation system [2].

On account of the rearrangement function needed in spectrum sensing and the fact that modulation recognition can provide reliable parameters for it, digital modulation recognition is of great importance in the whole system [3]. The goal of digital modulation recognition is to identify the modulation format of an unknown digital communication signal. For modulation classification, two general classes of classical methods exist: likelihood-based and feature-based methods, respectively [4, 5]. Based on the likelihood function of the received digital signal, the former method makes the decision by comparing the likelihood ratio with a threshold. In the feature-based method, several features are usually chosen and the decision is made jointly.

However, in traditional sensing process, two approaches are based on Shannon-Nyquist sampling theorem and the data scale to deal with can be enormous with a quite wide band especially in the cooperation networks. These years, researchers have brought compressive sensing (CS) in, which can solve the problem of high sampling rate caused by Shannon-Nyquist sampling theorem. It is declared that if the signal has a sparse representation in a fixed basis, we can reconstruct the sparse domain of the signal by solving an optimization algorithm, using samplings far fewer than dimensions of the original signal, and the original signal can be obtained by a simple matrix operation [6, 7].

In many CS conditions, we expect to acquire some signal characteristics rather than recovering the original signal, since reconstructing signals allows for lots of extra

operations, which results in higher complexity in both time and space. Researchers have already carried out much related valuable work in reconstructing signal characteristics based on CS [8, 9]. Inspired by these researches, we are devoted for finding identification features which can be used in the digital modulation recognition and simultaneously have sparsity, meaning they can be reconstructed directly by compressive samples.

In this paper, we propose a feature-based method based on CS for digital modulation recognition. We construct two identification features and use compressive samples to recover them directly, without recovering the original signals. One identification feature is the spectrum of received data and its nonlinear transformation, which is based on the feature proposed by [10], and the other is a compositional feature of multiple high-order moments of the received data. These two features can be used to identify various kinds of modulation modes, and, in this paper, we only focus on multiple frequency shift keying (MFSK), multiple phase shift keying (MPSK), and multiple quadrature amplitude modulation (MQAM). Simulations would be carried out to indicate that the performance of our method can be effective and reliable, with lower complexity and better antinoise property than traditional ones [11, 12].

The rest of this paper is organized as follows. Section 2 would present the system model adopted throughout the work, both the signal model and compressive sensing model. In Section 3, we construct two identification features and analysis sparsity of them. In Section 4, we build the linear relationships between identification features and compressive samples and give a brief introduction of the recovery method. Then, the whole recognition flowchart will be shown in Section 5. Simulations and analysis are present in Section 6. And, finally, we draw the conclusion in Section 7.

2. System Model

2.1. Signal Model. In a spectrum sensing scenario, we assume that a wide band received signal has one of the following modulation modes:

$$y(t) = \sum_{n=-\infty}^{n=\infty} Ag(t - nT) r(t) + v(t), \tag{1}$$

where A represents the amplitude of the received signal, T represents the symbol period, $g(t)$ represents the impulse response of pulse shaping low-pass filter, in which we choose rectangular pulse in this paper, and $v(t)$ stands for additive Gaussian white noise (AWGN). In the whole process, the timing offset and the carrier offset are both assumed to be zero, and the form of $r(t)$ is chosen as follows:

$$\begin{aligned} &\text{MPSK: } r(t) = e^{j(2\pi f_c t + 2\pi((i-1)/\beta))} \\ &\text{MFSK: } r(t) = e^{j(2\pi f_c t + 2\pi i \Delta f t)} \\ &\text{MQAM: } r(t) = \left(a_{i_c} + j a_{i_s}\right) e^{j2\pi f_c t} \\ &\qquad\qquad i \in \{2, 4, 8, \ldots, \beta\}, \end{aligned} \tag{2}$$

where f_c and β, respectively, stand for the carrier frequency and order of the chosen modulation mode, Δf is the carrier spacing, and $\{a_{i_c}\}$ and $\{a_{i_s}\}$ are a set of discrete levels. It is worth noting that there is no need of pulse shaping for MFSK, while in order to unity the form as (1), we regard $Ag(t - nT)$ in MFSK as 1, which would not influence the use of it.

2.2. Compressive Sampling Model. According to the theory of CS, the compressive sampling process can be modeled analytically as

$$\mathbf{z} = \mathbf{A}\mathbf{y}, \tag{3}$$

where $\mathbf{y}$ is the N-length sampling vector of the received signal $y(t)$ at a rate no lower than Nyquist sampling rate. $\mathbf{z}$ represents the subsampling measurements. $\mathbf{A}$ is a real-value measurement matrix of size $M \times N$, which complies with the restricted isometry property (RIP), such as Gaussian matrix, partial Fourier transform matrix, or others. In order to reconstruct the γth power of signal in Section 4.1, we adopt a special measurement matrix, with the value of "1" randomly located in each row and other elements being zero. Owing to the randomization of row elements, the matrix satisfies the RIP requirement as well as Gaussian matrix. Furthermore, the two-valued property of the matrix can enormously simplify the matrix operations, which make it possible to establish linear relationship between the nonlinear reconstruction target with the compressive samples.

To classify the modulated signal based on $\mathbf{z}$, we will firstly build the linear relationships between $\mathbf{z}$ and the identification features and then reconstruct the features directly with compressive samples $\mathbf{z}$ by solving an optimization algorithm, which would then be used to do digital modulation recognition.

3. Construction of the Identification Features

To achieve the goal of classifying modulation types accurately, identification features should be chosen with distinguishing details for each modulation type firstly. Secondly, identification features should have desired sparsity, in order to be constructed by compressive samples based on the theory of CS. According to these two requirements, we propose and construct the following two identification features.

3.1. Feature 1: Spectrum of the Signal's γth Power Nonlinear Transformation. Referring to [9], we calculate the Nth power of the received signal $y(t)$; that is,

$$[y(t)]^{\gamma} = \sum_{n=-\infty}^{n=\infty} A^{\gamma} g^{\gamma}(t - nT) r^{\gamma}(t) + v'(t), \tag{4}$$

where $\gamma = 2^k$ $(k = 0, 1, 2, \ldots)$. In the following, it will be shown that the spectrum of specific power order of signal level presents the recognizable characters for certain modulation types and orders. $v'(t)$ is the noise caused by nonlinear transformation of $v(t)$.

Then, we calculate the spectrum of $[y(t)]^{\gamma}$, which is represented as $\mathbf{y}^{\gamma}$, with γ ranging from 0 to a larger number. We have the following relationship:

$$\mathbf{y}^{\gamma} = \mathbf{F}\mathbf{S}_{\gamma}, \tag{5}$$

where $\mathbf{F} = [e^{-j2\pi ab/N}]_{(a,b)}$ represents the N-point IFFT matrix.

For different kinds of modulation modes, the results are quite different, which can be used to do the recognition, and we call this feature the spectrum feature below.

For MFSK, according to (1) and (2), the spectrum of it can be calculated as follows:

$$\begin{aligned}\mathbf{S}_{\mathrm{MFSK}} &= \int_{-\infty}^{\infty}\sum_{-\infty}^{\infty} Ae^{j(2\pi f_c t+2\pi i\Delta f t)}e^{-j2\pi ft}dt \\ &= A\sum_{i}\delta\left[f-(f_c+i\Delta f)\right],\end{aligned} \tag{6}$$

where $\delta(\cdot)$ stands for the impulse function. Obviously, there is impulse in the spectrum of MFSK, and the number of these impulses just corresponds to order β. As a contrast, the spectrum for MPSK can be presented as follows:

$$\begin{aligned}\mathbf{S}_{\mathrm{MPSK}} &= \int_{-\infty}^{\infty}\sum_{-\infty}^{\infty} Ag(t-nT)\,e^{j(2\pi f_c t+2\pi((i-1)/\beta))}e^{-j2\pi ft}dt \\ &= \sum_{i} A\sin c(f) * \delta(f-f_c)\,e^{j2\pi((i-1)/\beta)} \\ &= \sum_{i} A\sin c(f-f_c)\,e^{j2\pi((i-1)/\beta)},\end{aligned} \tag{7}$$

where $*$ stands for the convolution operation. The spectrum of MPSK comes out to be a monotone decreasing sine function, with no impulse. The calculation process of spectrum of MQAM is similar to MPSK, and their consequences are also similar. Figure 1 shows the results of different modulation types by $\gamma = 1$. From (a) and (b), we can see that there is apparent impulse for MFSK, just as we analyze in theory, quite different from that in (c) and (d), which represent the results of MPSK and MQAM, respectively. That is to say, we can distinguish MFSK from others by the spectrum of the signal, and the number of pulses indicates the order of MFSK.

For MPSK, when $\gamma < \beta$,

$$\begin{aligned}&\mathbf{S}_{\gamma\mathrm{MPSK}} \\ &= \int_{-\infty}^{\infty}\sum_{-\infty}^{\infty} A^{\gamma}g^{\gamma}(t-nT)\,e^{j\gamma(2\pi f_c t+2\pi((i-1)/\beta))}e^{-j2\pi ft}dt \\ &= \sum_{i} A^{\gamma}\sin c(f) * \delta(f-\gamma f_c)\,e^{j\gamma 2\pi((i-1)/\beta)} \\ &= \sum_{i} A^{\gamma}\sin c(f-\gamma f_c)\,e^{j\gamma 2\pi((i-1)/\beta)}.\end{aligned} \tag{8}$$

From the expression, we can see that there is no impulse in this condition. However, when $\gamma = \beta$,

$$\begin{aligned}&\mathbf{S}_{\beta\mathrm{MPSK}} \\ &= \int_{-\infty}^{\infty}\sum_{-\infty}^{\infty} A^{\beta}g^{\beta}(t-nT)\,e^{j\beta(2\pi f_c t+2\pi((i-1)/\beta))}e^{-j2\pi ft}dt \\ &= \int_{-\infty}^{\infty}\sum_{-\infty}^{\infty} A^{\beta}g^{\beta}(t-nT)\,e^{-j2\pi ft}dt \\ &= A^{\beta}\int_{-\infty}^{\infty} e^{-j2\pi ft}dt = A^{\beta}\delta(f).\end{aligned} \tag{9}$$

For $g(t-nT)$, we choose rectangle filter. Since $e^{j\beta(2\pi f_c t+2\pi((i-1)/\beta))} = 1$, $\sum_{-\infty}^{\infty} A^{\beta}g^{\beta}(t-nT)$ becomes a constant, and the Fourier transform of it is an impulse. Based on it, we compare the results of $\gamma = 1$, $\gamma = 2$, $\gamma = 4$, and $\gamma = 8$, referring to Figure 2. It can be seen that the impulse firstly appears when $\gamma = \beta$, with γ varying from small to big, which can be used to determine the order of MPSK.

As for MQAM, owing to similarity of the signal constellation, the property of MQAM is similar with QPSK, shown as Figure 3. It can be easily seen that the impulse firstly appears when $\gamma = 4$, and it has no relationship with the specific order of it.

The sparsity of this feature is in inverse proportion with N, which represents length of the signal as well as the IFFT size, on condition that there appears the impulse.

To sum up, the only remaining problem is to distinguish QPSK and MQAM. Therefore, we construct another feature for it.

3.2. Feature 2: A Composition of Multiple High-Order Moments of the Signal. For a digital modulated communication signal $x(m) = x(t) \mid (t = mTs,\ m = 1, 2, \ldots)$, the mixed moments of order $p+q$ are defined as (6), at a zero delay vector [10]:

$$M_{p+q,q}(x) = E\left(x(m)^{p}\left(x^{*}(m)\right)^{q}\right), \tag{10}$$

where the superscript $*$ denotes conjugation and $E(\cdot)$ means calculating the mean value.

In our system model, we intend to acquire $M_{2,1}(y)$ and $M_{4,0}(y)$ as recognition parameters, which we call the high-order moment feature.

With carrier known, symbols in the digital signals can be regarded as points in the signal constellation [13, 14]. Since points in digital signals of linear modulations are of equal probabilities, when the data size is large enough, we can use points in the signal constellation to calculate the theoretical values of $M_{2,1}$ and $M_{4,0}$, as Table 1 shows.

Referring to Table 1, $M_{4,0}$ of different modulation formats are of different theoretical times compared to E^2, which is the square value of $M_{2,1}$.

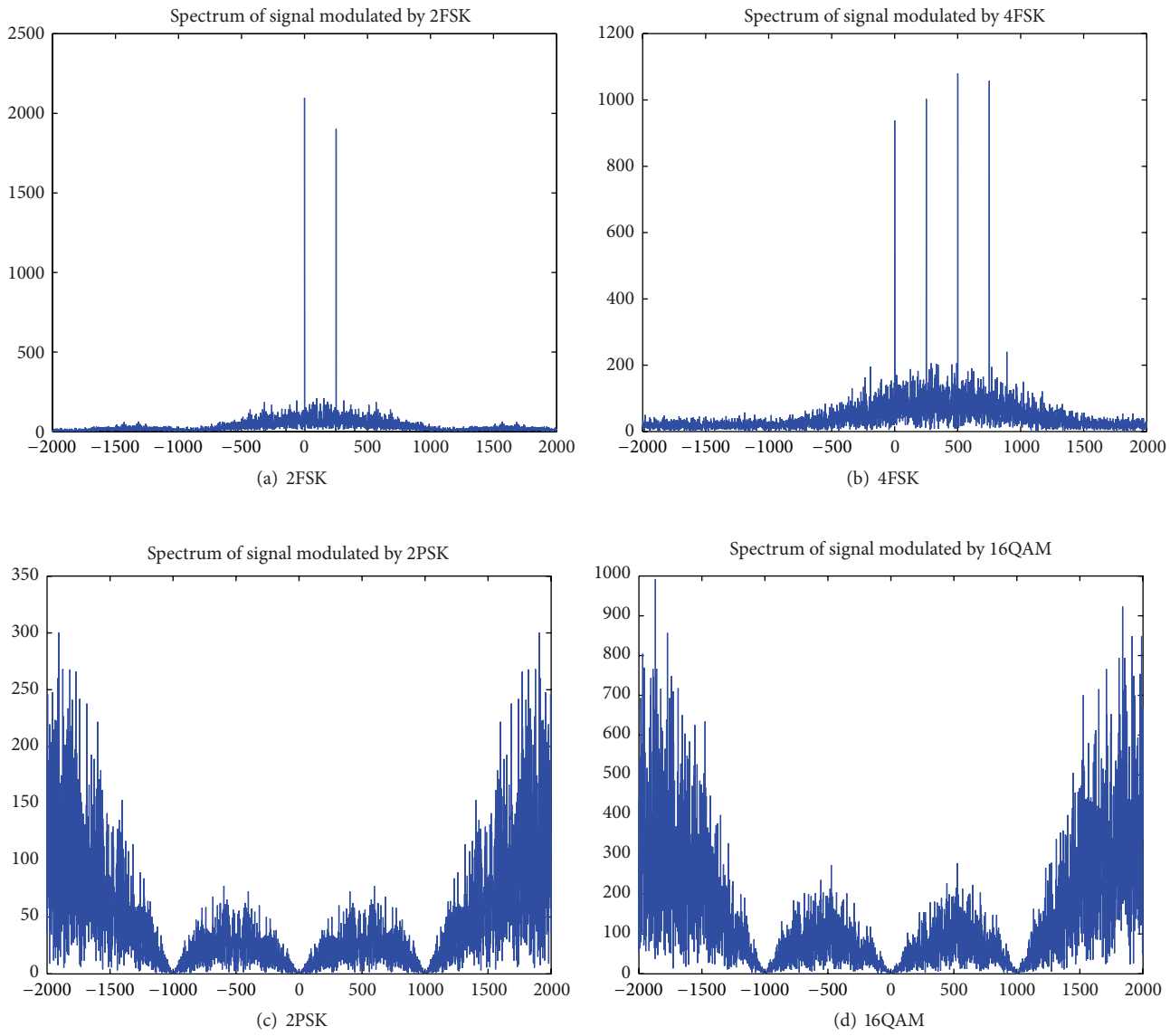

(a) 2FSK (b) 4FSK (c) 2PSK (d) 16QAM

Figure 1: Spectrum of different modulation modes.

We define the identification characteristic α in

$$\alpha = \left| \frac{M_{4,0}}{{M_{2,1}}^2} \right|. \tag{11}$$

We take QPSK and 16QAM as examples. According to (11), the theoretical values α of QPSK and 16QAM, respectively, come out to be 1 and 0.68. If we get the identification characteristic α of a signal, we can then identify the modulation format by comparing α with a suitable decision threshold.

Since high-order moment is a kind of statistics, we need sample several times. Then, to obtain $M_{2,1}(y)$ and $M_{4,0}(y)$, we construct matrixes as follows:

$$\mathbf{R}_{y21} = E\left(\mathbf{y}\mathbf{y}^H\right), \tag{12}$$

$$\mathbf{R}_{y40} = E\left(\mathrm{vec}\left\{\mathbf{y}\mathbf{y}^T\right\} \cdot \mathrm{vec}^T\left\{\mathbf{y}\mathbf{y}^T\right\}\right), \tag{13}$$

Table 1: Theoretical values of $M_{2,1}$ and $M_{4,0}$.

	$M_{2,1}$	$M_{4,0}$	${M_{4,0}}/{M_{2,1}}^2$
QPSK	E	$-E^2$	−1
8PSK	E	0	0
16QAM	E	$-0.68E^2$	−0.68

where $(\cdot)^H$ represents conjugate transpose, $(\cdot)^T$ represents transpose, and vec$\{\cdot\}$ stacks all columns of a matrix into a vector. For $\mathbf{R}_{y21}$, the element of matrix at row h, column k, is

$$r_{y_{21}}(h,k) = E\left(y_h {y_k}^*\right). \tag{14}$$

y_h, y_k are elements in the signal $\mathbf{y}$. When $h = k$, meaning diagonal elements, the values are equal to $M_{2,1}(y)$ based on the definition of high-order moments. However, when

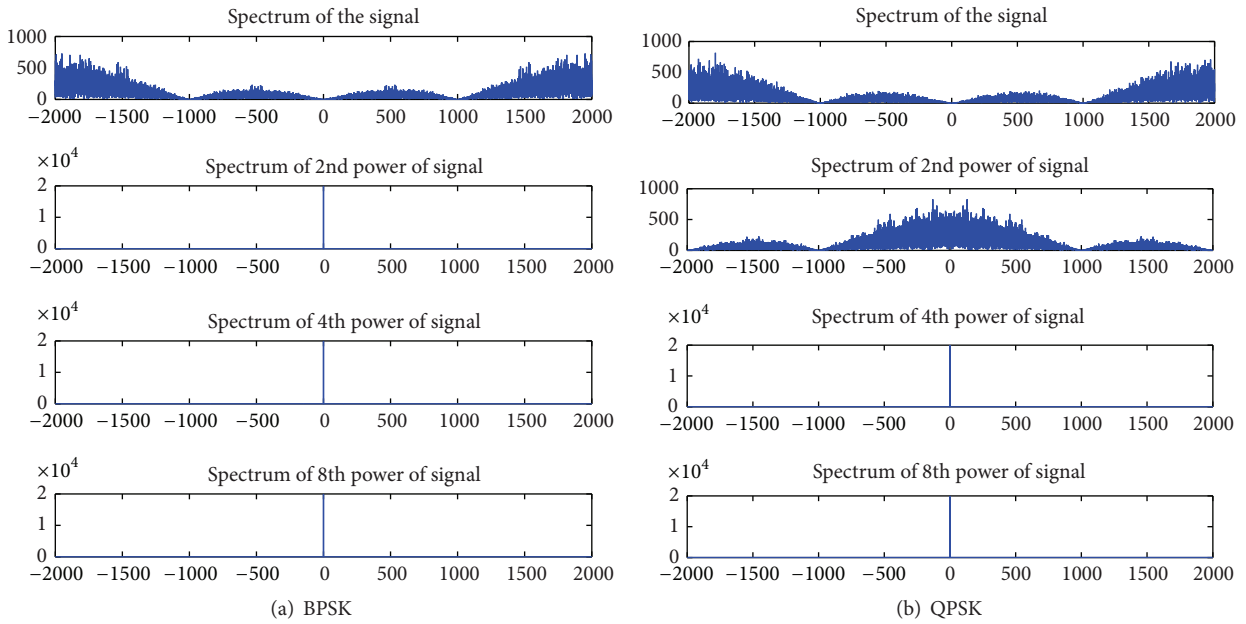

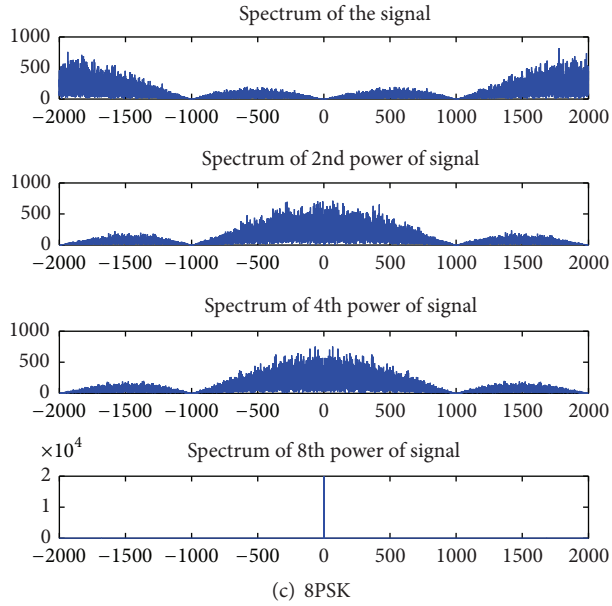

Figure 2: Spectrum of γth power of signal modulated by MPSK.

$h \neq k$, the value comes out to be zero for the uncorrelation between symbols of the signal. For $\mathbf{R}_{y40}$, $y_h y_k$ corresponds to $(N(h-1)+k)$th element of vec$\{\mathbf{y}\mathbf{y}^T\}$. When $h = k$, the relationship is that ${y_h}^2$ corresponds to the $(N(h-1)+h)$th element of vec$\{\mathbf{y}\mathbf{y}^T\}$. According to (10), $E({y_h}^4)$ is the desired value $M_{4,0}(y)$, so the $(N(h-1)+h)$th diagonal elements $(h = 1, 2, \ldots, N)$ of $\mathbf{R}_{y40}$ are equal to $M_{4,0}(y)$. Other elements are zero for the uncorrelation between symbols of the signal. The theoretical figures of $\mathbf{R}_{y21}$ and $\mathbf{R}_{y40}$ are shown as Figure 4.

It is obvious that $\mathbf{R}_{y21}$ and $\mathbf{R}_{y40}$ in Figure 4 are sparse. For $\mathbf{R}_{y21}$, all diagonal elements are nonzero, meaning the sparsity degree of it is $1/N$. For $\mathbf{R}_{y40}$, the $((h-1)\times N + h)$th elements of vec$\{\mathbf{R}_{x^T}\}$ are nonzero, meaning the sparsity degree of it is $1/N^3$.

4. Recovery of the Identification Features with Compressing Samples

In this section, we introduce the approaches of recovering the two identification features based on CS. We firstly build the linear relationships between compressive samples and the defined features and then give a brief introduction of the

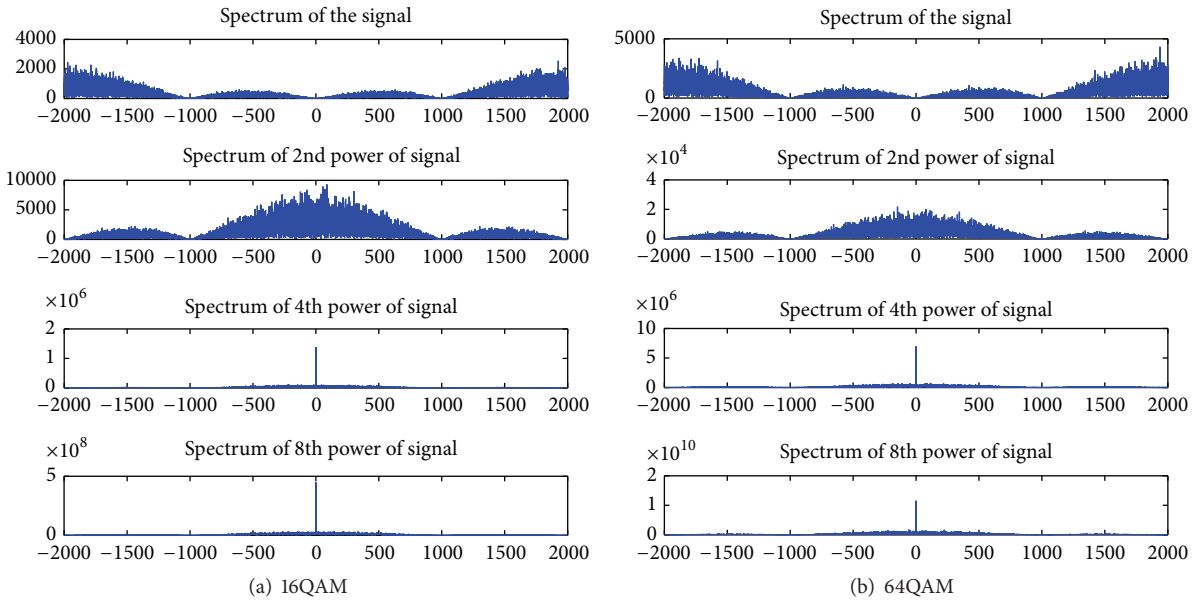

Figure 3: Spectrum of γth power of signal modulated by MQAM.

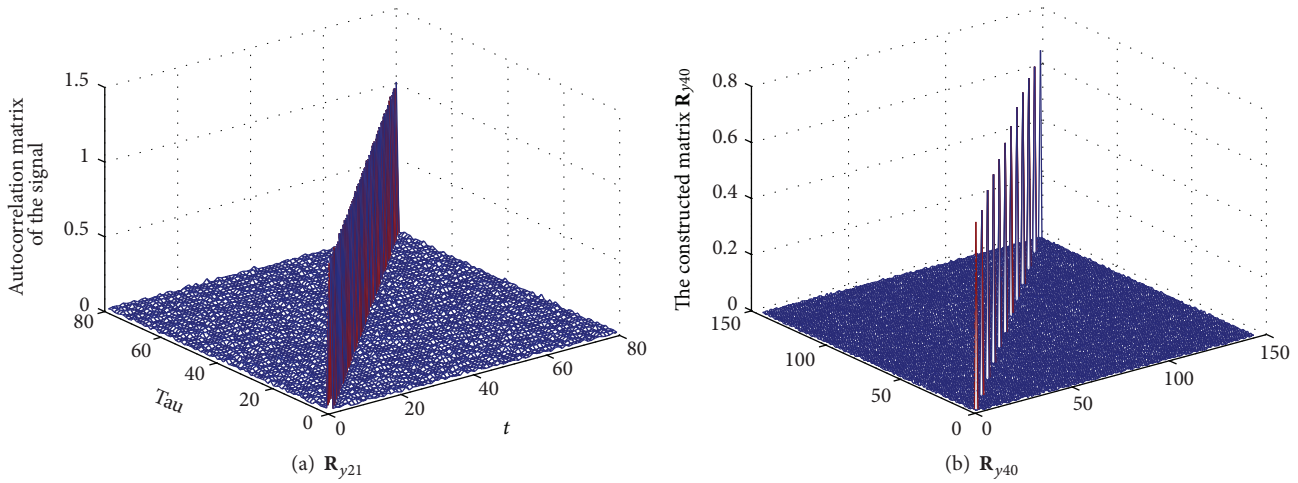

Figure 4: $\mathbf{R}_{y21}$ and $\mathbf{R}_{y40}$ of the signal modulated by 16QAM.

reconstruction algorithm and the practical selection strategy for the measurement matrix.

4.1. Linear Relationships between Compressive Samples and the Identification Features

4.1.1. Linear Relationships between Compressive Samples and the Spectrum Feature. It is obviously that the γth power of the signal is a nonlinear transformation. To get linear relationship between compressive samples and the spectrum of the signal's γth power nonlinear transformation, we choose the special measurement matrix proposed in Section 2. According to the nature of this certain-form matrix, we can easily get the following relationship based on (3):

$$\mathbf{z}^{\gamma} = \mathbf{A}_1 \mathbf{y}^{\gamma}, \tag{15}$$

and $\mathbf{A}_1$ is the measurement matrix for feature 1. Then, referring to (5), we obtain

$$\mathbf{z}^{\gamma} = \mathbf{A}_1 \mathbf{F} \mathbf{S}_{\gamma} = \mathbf{\Theta} \mathbf{S}_{\gamma}, \tag{16}$$

where $\mathbf{\Theta} = \mathbf{A}_1 \mathbf{F}$ is the sensing matrix we needed.

4.1.2. Linear Relationships between Compressive Samples and the High-Order Moment Feature. For this identification feature, the sampling matrix can be chosen as any one as long as it satisfies the restricted isometry property (RIP):

(i) $\mathbf{R}_{y21}$: according to (3) and the nature of transpose, we get the following relationship, and $\mathbf{A}_2$ stands for the measurement matrix for $\mathbf{R}_{y21}$:

$$\mathbf{z}\mathbf{z}^{H} = \mathbf{A}_2 \left(\mathbf{y}\mathbf{y}^{H}\right) {\mathbf{A}_2}^{H}. \tag{17}$$

Take the average of both sides:

$$E\left(\mathbf{z}\mathbf{z}^H\right) = \mathbf{A}_2 \cdot E\left(\mathbf{y}\mathbf{y}^H\right) \cdot {\mathbf{A}_2}^H. \tag{18}$$

We use $\mathbf{R}_{z21}$ to represent $E(\mathbf{z}\mathbf{z}^H)$, simultaneously refer to (12), and then get

$$\mathbf{R}_{z21} = \mathbf{A}_2 \cdot \mathbf{R}_{y21} \cdot {\mathbf{A}_2}^H. \tag{19}$$

Next, we apply the property $\text{vec}\{\mathbf{UXV}\} = (\mathbf{V}^T \otimes \mathbf{U})\text{vec}\{\mathbf{X}\}$ to transform (19) to (20). It is worth noticing that ${\mathbf{A}_2}^H = {\mathbf{A}_2}^T$, for $\mathbf{A}$ is a real-value matrix:

$$\text{vec}\left\{\mathbf{R}_{z21}\right\} = \mathbf{A}_2 \otimes \mathbf{A}_2 \text{vec}\left\{\mathbf{R}_{y21}\right\} = \mathbf{\Psi}\text{vec}\left\{\mathbf{R}_{y21}\right\}, \tag{20}$$

where $\mathbf{\Psi} = \mathbf{A}_2 \otimes \mathbf{A}_2$ can be regarded as the sensing matrix, with the scale of $M^2 \times N^2$.

(ii) $\mathbf{R}_{y40}$: since the sparsity degree of $\mathbf{R}_{y40}$ is far fewer than that of $\mathbf{R}_{y21}$, the dimension of signal needed and scale of measurement can also be very low. We represent the measurement for $\mathbf{R}_{y40}$ as $\mathbf{A}_3$, while the only difference of it from $\mathbf{A}_2$ is the dimension.

Similar to (17), there is

$$\mathbf{z}\mathbf{z}^T = \mathbf{A}_3 \left(\mathbf{y}\mathbf{y}^T\right) {\mathbf{A}_3}^T. \tag{21}$$

Then, according to $\text{vec}\{\mathbf{UXV}\} = (\mathbf{V}^T \otimes \mathbf{U})\text{vec}\{\mathbf{X}\}$, we can transform the two-dimensional relationship into one-dimensional relationship:

$$\text{vec}\left\{\mathbf{z}\mathbf{z}^T\right\} = \mathbf{A}_3 \otimes \mathbf{A}_3 \text{vec}\left\{\mathbf{y}\mathbf{y}^T\right\}. \tag{22}$$

We can obtain

$$\begin{aligned} &\text{vec}\left\{\mathbf{z}\mathbf{z}^T\right\} \text{vec}^T\left\{\mathbf{z}\mathbf{z}^T\right\} \\ &= \left(\mathbf{A}_3 \otimes \mathbf{A}_3\right) \text{vec}\left\{\mathbf{y}\mathbf{y}^T\right\} \text{vec}^T\left\{\mathbf{y}\mathbf{y}^T\right\} \left(\mathbf{A}_3 \otimes \mathbf{A}_3\right). \end{aligned} \tag{23}$$

Take the average of both sides:

$$\begin{aligned} &E\left(\text{vec}\left\{\mathbf{z}\mathbf{z}^T\right\} \text{vec}^T\left\{\mathbf{z}\mathbf{z}^T\right\}\right) \\ &= \left(\mathbf{A}_3 \otimes \mathbf{A}_3\right) E\left(\text{vec}\left\{\mathbf{y}\mathbf{y}^T\right\} \text{vec}^T\left\{\mathbf{y}\mathbf{y}^T\right\}\right) \left(\mathbf{A}_3 \otimes \mathbf{A}_3\right). \end{aligned} \tag{24}$$

Based on (13), we get the relationship:

$$\mathbf{R}_{z40} = \left(\mathbf{A}_3 \otimes \mathbf{A}_3\right) \mathbf{R}_{y40} \left(\mathbf{A}_3 \otimes \mathbf{A}_3\right), \tag{25}$$

where $\mathbf{R}_{z40}$ denotes $E(\text{vec}\{\mathbf{z}\mathbf{z}^T\}\text{vec}^T\{\mathbf{z}\mathbf{z}^T\})$. And then we have

$$\begin{aligned} \text{vec}\left\{\mathbf{R}_{z40}\right\} &= \left(\mathbf{A}_3 \otimes \mathbf{A}_3\right) \otimes \left(\mathbf{A}_3 \otimes \mathbf{A}_3\right) \text{vec}\left\{\mathbf{R}_{y40}\right\} \\ &= \mathbf{\Phi}\text{vec}\left\{\mathbf{R}_{y40}\right\}, \end{aligned} \tag{26}$$

where $\mathbf{\Phi} = (\mathbf{A}_3 \otimes \mathbf{A}_3) \otimes (\mathbf{A}_3 \otimes \mathbf{A}_3)$ is the sensing matrix.

4.2. Reconstruction of Identification Features. $\mathbf{z}^\gamma$, $\mathbf{R}_{z21}$, and $\mathbf{R}_{z40}$ can be calculated by the sampling value $\mathbf{z}$. With sensing matrixes and measurement vectors known, the reconstruction of the sparse vectors can be regarded as the signal recovery problem by solving the NP-hard puzzle as follows, taking $\mathbf{R}_{y21}$ as an example:

$$\begin{aligned} \widetilde{\text{vec}\left\{\mathbf{R}_{y21}\right\}} = \arg\min \quad & \left\|\text{vec}\left\{\mathbf{R}_{y21}\right\}\right\|_0 \\ \text{s.t.} \quad & \text{vec}\left\{\mathbf{R}_{z21}\right\} = \mathbf{\Phi}\,\text{vec}\left\{\mathbf{R}_{z21}\right\}. \end{aligned} \tag{27}$$

This can be transformed into a linear programming problem:

$$\begin{aligned} \min_{\widetilde{\text{vec}\{\mathbf{R}_{y21}\}}} & \left\|\text{vec}\left\{\mathbf{R}_{z21}\right\} - \mathbf{\Phi}\,\text{vec}\left\{\mathbf{R}_{y21}\right\}\right\|_2^{1/2} \\ & + i\left\|\text{vec}\left\{\mathbf{R}_{y21}\right\}\right\|_1 \end{aligned} \tag{28}$$

which is called $l1$-norm least square programming problem and is proved to be convex that there exists a unique optimum solution. $i > 0$ is a weighting scalar that balances the sparsity of the solution induced by the $l1$-norm term and the data reconstruction error reflected by the $l2$-norm LS term.

In Section 4.1, we have mentioned recovering three recognition features by using measurement matrixes $\mathbf{A}_1$, $\mathbf{A}_2$, and $\mathbf{A}_3$, respectively. However, practically, only using $\mathbf{A}_1$ as the compressive measurement may meet the requirement of recovering all of the features. The reason is that $\mathbf{A}_2$ and $\mathbf{A}_3$ differ in the dimension but are both designed with the constraint of RIP property only. From the other aspect, the primary requirement of constructing matrix $\mathbf{A}_1$ is also the RIP condition.

5. Modulation Recognition with the Identification Features

Given a received communication signal modulated by MFSK, MPSK, or MQAM, we firstly get compressive samples using measurement matrixes present in Section 2. In this process, due to difference of sparsity we have analyzed in Section 3, various features may apply various length of the signal, and this can be decided based on actual situations. According to the approaches proposed above, the identification features can be easily obtained. Then, we can recognize the modulation format effectively referring to the flowchart shown in Figure 5, and specific steps are listed in the following.

Step 1. Reconstruct the spectrum feature when $\gamma = 1$ with compressive samples. If there is impulse in the recovered spectrum, the modulation mode can be identified as MFSK, and the number of impulses indicates the order of it. However, if there is no impulse in the feature, the communication signal is modulated by MPSK or MQAM, and then Step 2 should be conducted.

Step 2. Reconstruct the spectrum feature when $\gamma = 2, 4, 8, \ldots$ with compressive samples and observe value of γ when the impulse firstly appears. If $\gamma = 4$ when the impulse appears, the modulation mode can be regarded as QPSK or MQAM,

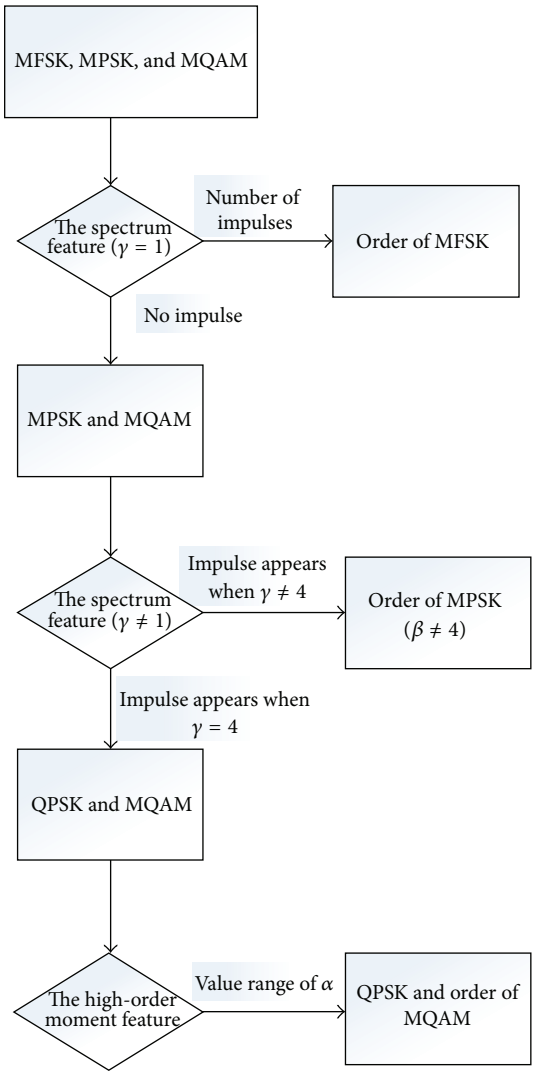

Figure 5: The process of digital modulation recognition.

and then we go to Step 3. However, if $\gamma \neq 4$ when the impulse appears, the signal is modulated by MPSK and this value of γ is the order of it.

Step 3. Reconstruct $\mathbf{R}_{y21}$ and $\mathbf{R}_{y40}$ of the signal with compressive samples, get average values of the diagonal as $M_{2,1}(y)$ and $M_{4,0}(y)$, respectively, and then calculate α based on (11). Compare α with the calculated boundary values shown in Table 1 and determine the modulation type.

6. Numerical Results

This section presents the simulation results of our feature-based recognition method. We firstly generate a stream of signals modulated by MPSK, MFSK, or MQAM. All the signals share the same bit rate 1 kbit/s and the carrier frequency 2 kHz, and the carrier spacing for MFSK is 0.25 kHz. For the two proposed features, the observation time is various because data volume needed by the two features are all

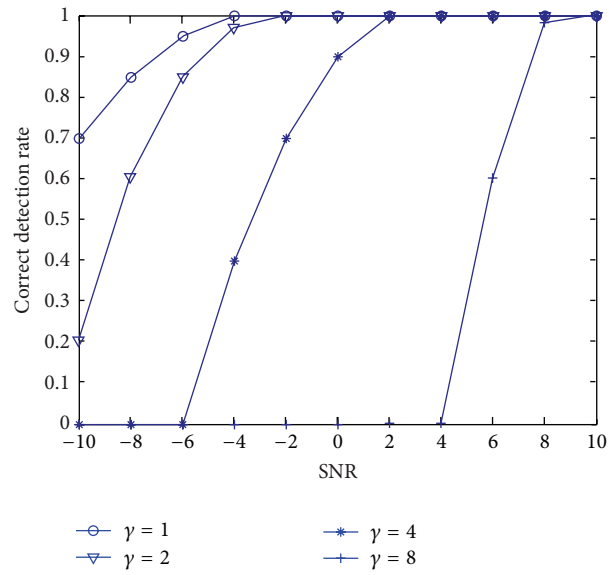

Figure 6: Correct detection rate of impulse in reconstructed feature 1.

different. The performance of reconstruction is closely related to the signal-to-noise ratio (SNR), which is set as a variable in our simulation, and simulations at every SNR are carried out for 500 times.

As mentioned above, information we need to capture in feature 1 is whether there are impulses and the number of them, rather than accurate numerical values. Therefore, we apply correct detection rate of pulse to evaluate the performance of reconstruction of spectrum feature, which is shown in Figure 6. We set a decision threshold which equals two-thirds of the biggest reconstructed value, and if there is no other value larger than the threshold, the biggest value would be regarded as the impulse. In this scenario, the compressive ratio is set as 0.3, which means $M/N = 0.3$. We calculate the detection rate for MFSK signal on $\gamma = 1$, BPSK on $\gamma = 2$, QPSK and MQAM on $\gamma = 4$, and 8PSK on $\gamma = 8$, respectively. It is obvious that the detection rate varies a lot with γ. The reason is that γth power of signal is a nonlinear transform, meaning that the uniformly distributed noise is magnified, and the degree of magnification extends as the increasing of γ. Therefore, detection rate of impulse when $\gamma = 8$ is the worst one.

Figure 7 shows the mean square error (MSE) of reconstructed feature 2 with respect to the theoretical ones. That is,

$$\mathrm{MSE} = E\left\{\frac{\left\|\widetilde{\mathrm{vec}\left\{\mathbf{S}_\gamma\right\}} - \mathrm{vec}\left\{\mathbf{S}_\gamma\right\}\right\|_2^2}{\left\|\mathrm{vec}\left\{\mathbf{S}_\gamma\right\}\right\|_2^2}\right\}. \tag{29}$$

We give the MSE of reconstructed $\mathbf{R}_{y21}$ and $\mathbf{R}_{y40}$, respectively, with the compressive ratio chosen as 0.3 and 0.45. From Figure 7, we can see that the performance of reconstruction of $\mathbf{R}_{y40}$ is closely related to the compressive ratio, while the performance of reconstruction of $\mathbf{R}_{y21}$ is relatively perfect

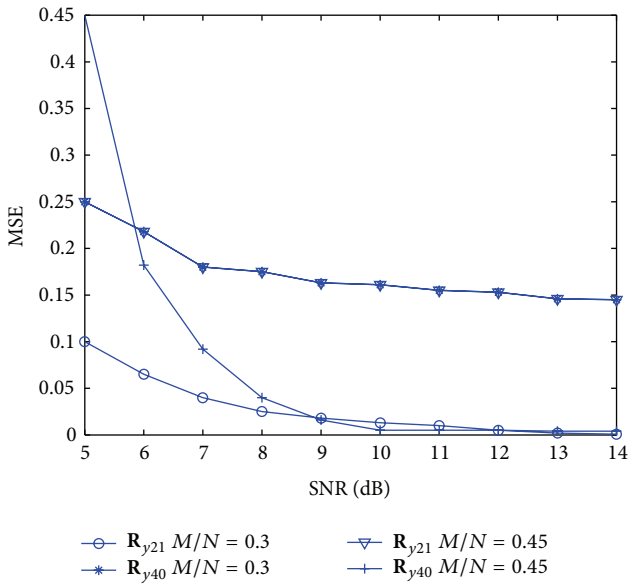

FIGURE 7: MSE of reconstructed $\mathbf{R}_{y21}$ and $\mathbf{R}_{y40}$ with different compressive ratio.

even at a low compressive ratio. Moreover, we can easily get the conclusion that when the compressive ratio is suitable, the precision of feature 2 is high enough as long as the SNR is higher than 10 dB.

Figure 8 shows the correct classification rate of different modulation modes at relatively low SNR. Difference of the correct classification comes from various performance of reconstruction of features, which has been shown in Figures 6 and 7. MFSK has high recognition rate, larger than 0.93 even when SNR = −6 dB. For MPSK, the correct recognition rate declines as β increases. However, for QPSK and MQAM, the performance is quite different, and we give the following analysis.

According to [14], we have the fact that $M_{4,0}$ of just the signal and mixture of noise and signal are of the same value, so the main cause of the error comes from $M_{2,1}$.

As for $M_{2,1}$, we have the following proof stating the variation of the value in noisy condition and noiseless condition. To describe this clearly, $M_{2,1}(y_0)$, $M_{2,1}(v)$, and $M_{2,1}(y)$ are, respectively, used to replace $M_{2,1}$ while being in the following condition of signal only, noise only, and the mixture of noise and signal:

$$\begin{aligned} M_{2,1}(y_0) &= E(y_{0h}{y_{0h}}^*), \\ M_{2,1}(v) &= E(v_h{v_h}^*), \\ M_{2,1}(y) &= E\left((y_{0h}+v_h)(y_{0h}+v_h)^*\right) \\ &= E\left((y_{0h}+v_h)({y_{0h}}^*+{v_h}^*)\right) \\ &= E\left(y_{0h}{y_{0h}}^* + {y_{0h}}^*v_h + y_{0h}{v_h}^* + v_h{v_h}^*\right) \\ &= E(y_{0h}{y_{0h}}^*) + E({y_{0h}}^*v_h) + E(y_{0h}{v_h}^*) \\ &\quad + E(v_h{v_h}^*). \end{aligned} \tag{30}$$

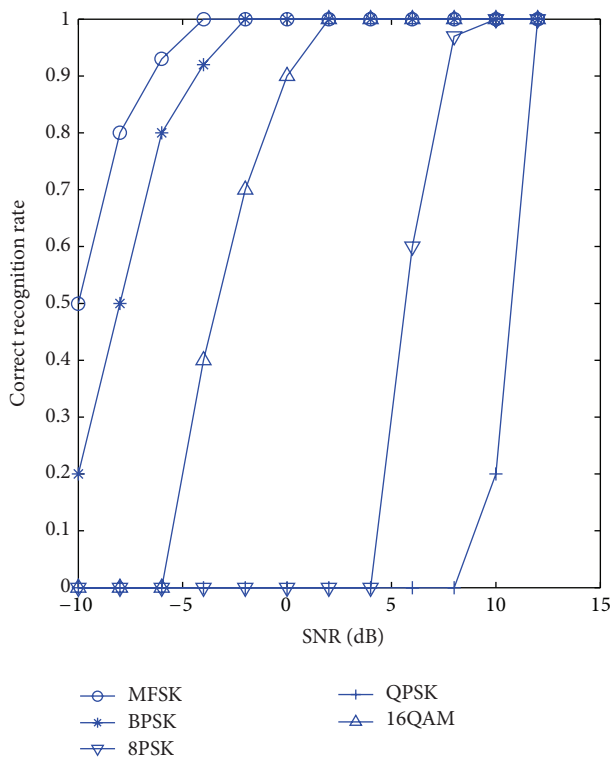

FIGURE 8: Correct classification rate of different modulation modes.

v is zero-mean random measure noises with Gaussian distribution, which is independent from y. According to the nature of expectation, we know that

$$E({y_{0h}}^*v_h) = E(y_{0h}{y_{0h}}^*) = 0. \tag{31}$$

Therefore, we can obtain the following relationship:

$$\begin{aligned} M_{2,1}(y) &= E(y_{0h}{y_{0h}}^*) + E(v_h{v_h}^*) \\ &= M_{2,1}(y_0) + M_{2,1}(v) \end{aligned} \tag{32}$$

meaning $M_{2,1}(y)$ is the sum of signal power and noise power.

From (11) and (27), we can obtain the relationship of the theoretical α and the actual α':

$$\begin{aligned} \alpha &= \left|\frac{M_{4,0}(y_0)}{{M_{2,1}}^2(y_0)}\right|, \\ \alpha' &= \left|\frac{M_{4,0}(y)}{{M_{2,1}}^2(y)}\right| = \left|\frac{M_{4,0}(y_0)}{{M_{2,1}}^2(y_0)+{M_{2,1}}^2(v)}\right| \\ &= \left|\frac{M_{4,0}(y_0)}{{M_{2,1}}^2(y_0)\left(1+{M_{2,1}}^2(v)/{M_{2,1}}^2(y_0)\right)}\right| \\ &= \frac{P_v}{P_v+P_{y_0}}\alpha, \end{aligned} \tag{33}$$

where P_v denotes noise power and P_{y_0} denotes signal power.

To sum up, $M_{2,1}(y)$ is added by the power of noise, and, as a consequence, the identification parameter α becomes

smaller; thus, QPSK may be recognized as 16QAM. Therefore, the correct recognition rate of 16QAM is much higher than QPSK when SNR is lower than 10 dB, as shown in Figure 8.

7. Conclusion

To solve the problem of high sampling rate for digital modulation recognition in spectrum sensing, we have proposed a feature-based method to identify the modulation formats of digital modulated communication signals using compressive samples and have greatly lowered the sampling rate based on CS. Two features are constructed in our method, one of which is the spectrum of signal's γth power nonlinear transformation, and the other is a composition of multiple high-order moments of the signal, both with desired sparsity. By these two features, we have applied suitable measurement matrixes and built linear relationships referring to them. The method successfully avoids reconstructing original signals and uses recognition features to classify signals directly, declining the algorithm complexity effectively. Simulations show that correct recognition rates are different for different modulation types but are all relatively ideal even in noisy scenarios. In actual situations, the method can be decomposed aiming at variable demands, and, for further work, we tend to improve the performance of the whole method continuously, especially the noise elimination in the classification of QPSK and MQAM.

Conflict of Interests

The authors declare that there is no conflict of interests regarding the publication of this paper.

Acknowledgments

This work was supported by The China National Natural Science Fund, under Grants 61271181 and 61171109, and the Joint Project with China Southwest Institute of Electronic and Telecommunication Technology.

References

[1] H. Bogucka, P. Kryszkiewicz, and A. Kliks, "Dynamic spectrum aggregation for future 5G communications," *IEEE Communications Magazine*, vol. 53, no. 5, pp. 35–43, 2015.

[2] T. Irnich, J. Kronander, and Y. Selen, "Spectrum sharing scenarios and resulting technical requirements for 5G systems," in *Proceedings of the IEEE 24th International Symposium on Personal, Indoor and Mobile Radio Communications (PIMRC Workshops '13)*, pp. 127–132, IEEE, London, UK, September 2013.

[3] S. Fengpan, *Research on Modulation Classification for Compressive Sensing in Cognitive Radio*, Ningbo University, 2013.

[4] O. A. Dobre, A. Abdi, Y. Bar-Ness, and W. Su, "Survey of automatic modulation classification techniques: classical approaches and new trends," *IET Communications*, vol. 1, no. 2, pp. 137–156, 2007.

[5] F. Wang and X. Wang, "Fast and robust modulation classification via Kolmogorov-Smirnov test," *IEEE Transactions on Communications*, vol. 58, no. 8, pp. 2324–2332, 2010.

[6] E. Cands, "Compressive sampling," in *Proceedings of the International Congress of Mathematicians*, vol. 3, pp. 1433–1452, Madrid, Spain, 2006.

[7] E. J. Candes and M. B. Wakin, "An introduction to compressive sampling," *IEEE Signal Processing Magazine*, vol. 25, no. 2, pp. 21–30, 2008.

[8] Z. Tian, Y. Tafesse, and B. M. Sadler, "Cyclic feature detection with sub-nyquist sampling for wideband spectrum sensing," *IEEE Journal on Selected Topics in Signal Processing*, vol. 6, no. 1, pp. 58–69, 2012.

[9] L. Zhou and H. Man, "Distributed automatic modulation classification based on cyclic feature via compressive sensing," in *Proceedings of the IEEE Military Communications Conference (MILCOM '13)*, pp. 40–45, IEEE, San Diego, Calif, USA, November 2013.

[10] J. Reichert, "Automatic classification of communication signals using higher order statistics," in *Proceedings of the IEEE International Conference on Acoustics, Speech and Signal Processing (ICASSP '92)*, vol. 5, pp. 221–224, San Francisco, Calif, USA, March 1992.

[11] V. Orlić and M. L. Dukić, "Algorithm for automatic modulation classification in multipath channel based on sixth-order cumulants," in *Proceedings of the 9th International Conference on Telecommunication in Modern Satellite, Cable, and Broadcasting Services (TELSIKS '09)*, pp. 423–426, IEEE, Niš, Serbia, October 2009.

[12] D. C. Chang and P. K. Shih, "Cumulants-based modulation classification technique in multipath fading channels," *IET Communications*, vol. 9, no. 6, pp. 828–835, 2015.

[13] B. Wang and L. Ge, "A novel algorithm for identification of OFDM signal," in *Proceedings of the International Conference on Wireless Communications, Networking and Mobile Computing (WCNM '05)*, pp. 261–264, September 2005.

[14] D. Grimaldi, S. Rapuano, and G. Truglia, "An automatic digital modulation classifier for measurement on telecommunication networks," in *Proceedings of the IEEE Instrumentation and Measurement Technology Conference—Conference Record*, pp. 1711–1720, Sorrento, Italy, 2002.